Near infrared hyperspectral imaging for deoxynivalenol and ergosterol estimation in wheat samples

Antoni Femenias[a], Ferran Gatius[b], Antonio J. Ramos[a], Vicente Sanchis[a], Sonia Marín[a*]

[a]Applied Mycology Unit, Food Technology Department, University of Lleida, Agrotecnio center, Av. Rovira Roure 191, 25198, Lleida, Spain

[b] Department of Chemistry, University of Lleida (UdL), Av. Rovira Roure, 191, Lleida, 25198, Spain

Corresponding author:

Sonia Marín Sillue

Food Technology Department, University of Lleida

Av. Rovira Roure 191, 25198, Lleida, Spain

Tel: (+34) 973 70 25 42

Fax: (+34) 973 70 25 96

Email: smarin@tecal.udl.cat

ABSTRACT

The present study aimed to evaluate the use hyperspectral imaging (HSI)-NIR spectroscopy to predict DON and ergosterol concentration through high-accuracy prediction and classification models to quantify DON and to classify samples according to EU maximum limit (1250 μg/kg). To achieve these objectives, a first set of bulk samples was scanned by HSI-NIR and divided into two subsamples in which one was analysed for ergosterol and the other for DON by HPLC. The method was repeated for a second larger set to build prediction and classification models. All the spectra were pretreated and statistically processed by PLSR and LDA. Prediction models presented RMSEP of 1.17 mg/kg and 501 μg/kg for ergosterol and DON, respectively. Classification achieved an encouraging accuracy of 85.4% for an independent validation set of samples. The results confirm that HSI-NIR may be a suitable technique for DON quantification and classification, although ergosterol was inappropriate for DON indirect detection.

Keywords: Hyperspectral imaging; Deoxynivalenol; Ergosterol; Near infrared; Cereal analysis.

Nomenclature

FHB	Fusarium Head Blight
DON	Deoxynivalenol
HPLC	High Performance Liquid Chromatography
ELISA	Enzyme-Linked Immunosorbent Assays
LFD	Lateral Flow Devices
NIRS	Near Infrared Spectroscopy
HSI	Hyperspectral imaging
EU	European Union
DPI	DON Preliminary Index

SVM	Support Vector Machine
PLS	Partial Least Squares
DA	Discriminant Analysis
LDA	Linear Discriminant Analysis
IAC	Immunoaffinity Chromatography
ROI	Region of Interest
UHPLC-DAD	Ultra High Performance Liquid Chromatography – Diode Array Detector
Vis	Visible range
PCA	Principal Component Analysis
RMSECV	Root Mean Square Error of Cross-Validation
R_{cv}^2	Coefficient of determination of cross-validation
RMSEP	Root Mean Square Error of Prediction
R_v^2	Coefficient of determination of validation
PC	Principal Components
SEP	Standard Error of Prediction
ABS/BC	Baseline Corrected Absorbance Spectra
1stD	1st Derivate spectra
FDK	*Fusarium* Damaged Kernels
FT-NIR	Fourier-Transformed Near Infrared
MSC	Multiplicative Scatter Correction
SPA	Successive Projections Algorithm
SVM	Support Vector Machines

1. INTRODUCTION

Fusarium is a plant pathogen extensively present in wheat that produces diseases causing the loss of harvest yield, crop quality and economic value. One of the most important diseases caused by these fungi is Fusarium head blight (FHB), which affects spikes causing shrivelling, weight loss and discoloration of kernels (Beyer, Pogoda, Ronellen, Hoffmann, & Udelhoven, 2010). Moreover, under suitable environmental conditions of temperature, water activity, pH and nutrient availability it is able to produce deoxynivalenol (DON), which is a mycotoxin that causes negative effects to human and animal health. Ineffective approaches for DON reduction in preharvested wheat and its resistance to food processing methods make DON a high prevalence toxin in food chain (Pestka, 2010). For these reasons, efficient strategies to discern between contaminated and toxin-free wheat batches prior to food chain entry are needed.

Well-known strategies such as HPLC and enzyme-linked immunosorbent assays (ELISA) are extensively used for DON detection and quantification in cereal grains. However, time-consume is one of the most important shortcomings of these techniques. Consequently, rapid techniques for detection and measurement of DON are demanded by companies for their monitoring prior to enter in food industry, such as lateral flow devices (LFD). At the moment, spectroscopic techniques are promising not only for their rapid analysis power, but also because they are environmental-friendly, cost-effective and non-destructive. Near infrared spectroscopy (NIRS) has been already used for the determination of majority components present in food, such as protein, moisture, structural carbohydrates and fats (Caporaso, Whitworth, & Fisk, 2018; Pandey, Srivastava, & Mishra, 2018). The application of this technique to minority pollutants, as DON, has been investigated by many authors. Some studies have also evaluated the influence of ergosterol in the NIR spectra for its determination and prediction in relation with the *Fusarium* growth and damage (Dowell, Ram, & Seitz, 1999; Mancinelli, Costantini, & Rossi, 2014). Ergosterol is a predominant chemical component of the fungi cell membrane. At the same time, it is a minor or absent component in most plants and consequently it indicates the presence of fungal growth in cereal products (Seitz, 1979).

Hyperspectral imaging (HSI) is a novel approach that presents improvements on the conventional NIR devices. Its main advantage is that it provides spectral information of each pixel of the captured image. Thus, it is a high-performance analytical device, especially in heterogeneous samples. The most appropriate spectrometry technology for grain evaluation is the diffuse reflectance which is able to partially penetrate into the sample to show their physical and chemical characteristics (Fox & Manley, 2014). In addition, the push broom imaging is the most widely used technique for HSI recording. This measurement mode is based on the scanning through the 'y' axis for the recording of NIR spectra of each pixel of the 'x' dimension for all its wavelength range (Boldrini, Kessler, Rebnera, & Kessler, 2012).

Several studies tested the HSI spectroscopy for *Fusarium* damage assessment. Most of them used the visual inspection as the reference method for HSI calibration, in which kernel symptoms have been used for kernel classification (Delwiche, Kim, & Dong, 2011; Ropelewska & Zapotoczny, 2018; Serranti, Cesare, & Bonifazi, 2013). Otherwise, ergosterol has not been extensively used for HSI calibration. However, as the ergosterol is considered an indicator of fungal growth (Magan, 1993), some authors used this chemical compound for the estimation of fungal damage in cereals (Börjesson, Stenberg, & Schnürer, 2007; Delwiche et al., 2011; Dowell et al., 1999). In addition, the influence of ergosterol on the spectra near the 1200 nm band has also been studied (Delwiche et al., 2011; Delwiche, Rodriguez, Rausch, & Graybosch, 2019; Femenias, Gatius, Ramos, Sanchis, & Marín, 2020). Consequently, an ergosterol calibration for a rapid determination of fungal growth would be an improvement to the visual inspection, which is an imprecise and qualitative method. Moreover, a well-fitted ergosterol prediction model in which the fungal alteration of wheat is evaluated, could be used as an indirect method for DON contamination estimation.

Likewise, HSI-NIR has been used for rapid DON detection and quantification in wheat. Barbedo, Tibola, & Fernandes (2015) focused on the correlation between the visual symptoms and DON concentration by a *Fusarium* index determination in which they demonstrated that visual symptoms are not totally correlated with DON contamination. A subsequent study

(Barbedo, Tibola, & Lima, 2017) aimed to classify wheat samples into two (above or under the EU limit, 1250 µg/kg) and three groups (< 500 µg/kg; 500-1250 µg/kg; > 1250 µg/kg) using a confusion matrix. In this report, a DON preliminary index (DPI) was used to obtain notable classification accuracies above 70 %, although, due to its low correlation (0.54) with DON concentration, a prediction model was not explored. Moreover, Liang et al. (2018) also classified wheat samples according to DON mean concentrations into three groups (< 250 µg/kg; 1162 µg/kg; 2665 µg/kg) using a high complexity model by the combination of Support Vector Machine (SVM) and Partial Least Squares – Discriminant Analysis (PLS-DA). Recently published studies determined a positive correlation between the spectral signatures of wheat kernels and wheat flour and fungal DNA and DON content (Alisaac et al., 2019).

In order to contribute to the performance improvement of the fungal and DON contamination prediction, this study aimed to develop an enhanced predictive method. Firstly, HIS-NIR spectroscopy was used to attempt the indirect determination of DON, first by evaluating the coefficient of determination of ergosterol which could explain DON and then by the calibration of an ergosterol predictive model as indicator to fungal presence. Secondly, using a considerable number of samples compared to other studies with similar purposes, DON quantification and classification of wheat samples according to the established EU limit by HSI-NIR analysis was carried out. PLS and LDA were used as the multivariate statistical techniques to reach these objectives (Esbensen, Swarbrick, Westad, Whitcombe, & Anderson, 2018).

2. MATERIALS AND METHODS

2.1. Determination of ergosterol and DON concentration in wheat samples by UHPLC

2.1.1. Reagents and chemicals

Water was obtained from a Milli-Q® SP Reagent water system from Millipore Corp. (Brussels, Belgium). Methanol and acetonitrile (HPLC grade) were purchased from Scharlab (Sentmenat, Spain). Mycotoxin standards of DON were purchased from Romer Labs (Tulln, Austria).

Immunoaffinity chromatography (IAC) columns for DON (DONPREP®) were acquired from R-Biopharm (Rhone LTD Glasgow, UK). Potassium hydroxide was obtained from VWR Prolabo (Geldenaaksebaan, Leuven) and n-hexane was purchased from VWR BDM Prolabo (Fontenay-sous-Bois, France). Mycotoxin standards of DON was purchased from Romer Labs (Tulln, Austria) and ergosterol was acquired from Sigma (St. Louis, Mo).

2.2. HIS-NIR experimental work

Instrumentation and data acquisition by HSI-NIR

A push-broom hyperspectral imaging system composed by a Pika NIR-320 camera assembled in RESONON Inc. (Boezman, MA, USA) was used. The device consists in an InGaAS sensor line scan camera with 320×256-pixel resolution, a 30×30 μm pixel size, a 14-bit resolution A/D spectrograph (Goldeye G-008 SWIR TEC1, Allied Vision Technologies GmbH, Germany). The spectral resolution is 4.9 nm (164 spectral bands from 900 to 1700 nm), with 320 pixels of spatial resolution and frame rate of 520 fps. The objective lens has 25 mm of focal length (F/1.4 SWIR, 0.9-1.7 μm, 21 mm image format, c-mount) and are positioned 220 mm above the image surface. Illumination unit is composed by a four halogen lamps lighting system with Lambertian filters fixed on an adjustable tower that are turned on at least 20 min before the image acquisition. The illumination system was powered by Samplexpower® power converter (SEC-1223CE, Burnaby, BC, V5A 0C6, Canada) which provides a highly regulated output DC voltage of 13.8 Volts at 23 Amps with an AC input of 230 Volts, 50 Hz. Finally, a motorized linear translation stage of 600 mm was also used, which permitted the scan of the full sample having the optical systems fixed.

The Spectronon PRO software was used to control Resonon's benchtop for the image processing. The intensity readings of each test sample data array were automatically transformed to reflectance by dividing the dark current-subtracted intensity by the dark current-subtracted white standard intensity at each of the corresponding wavelengths (1). A dark current intensity image was collected before samples' scanning to remove dark current noise by covering the camera lens. Likewise, intensity from a 99% white reflectance standard, made of

polytetrafluoroethylene (Spectralon™, SRT-99-120, Labsphere, North Sutton, NH, USA) to correct illumination effects, was collected immediately after the dark current image. These two images were applied to the subsequent sample intensity images.

$$I = \frac{I_0 - I_b}{I_w - I_b} \quad (1)$$

where I_0 is the raw hyperspectral image obtained, I_w is the white reference and I_b is the dark current reference. In addition to dark and absolute reflectance response, the pixel illumination saturation was also adjusted by the camera controls. Framerate and integration time were established so that no pixel on the image was saturated.

The work was divided in two trials. In the first one, 14 g of wheat kernels were scanned without any specific template. Mean spectrum of the bulk sample was recorded. This process was repeated in triplicate, shaking between each scanning, to obtain a change in the kernel orientation of the whole sample and representative spectra of its characteristics. Once the spectra were recorded, the samples were ground with an IKA® A11 Basic mill (Darmstadt, Germany). Ground wheat obtained in each sample (14 g) was scanned in the same way as for the whole kernels. After these two steps, each sample was divided into two equal parts of 7 g, one for ergosterol extraction and the other for DON extraction. The second trial was also divided in two steps, in the first, 14 g of bulk wheat kernels were scanned in triplicate. The samples were ground as in the first trial and the resulting product was scanned for three times. In this case, the 14 g were entirely used for DON extraction.

In all cases, a black tray was used to reduce the background noise on the image and to obtain an accurate pixel selection. Images were adjusted to 350 bands for horizontal size and approximately 90 mm of vertical size. The pixel selection was done by the collection of the mean reflectance's of similar spectrum pixels by Euclidian distance that are best adjusted to the region of interest (ROI) to remove the background signal. Mean spectra for full samples were recorded as text file for their subsequent exporting to the spectral analysis software.

2.3. Preparation of ergosterol solutions

Standard solutions were prepared dissolving 20 mg of ergosterol in 10 mL of dissolvent (dicloromethane:isopropanol, 99:1, v/v). 3 mL of the solution were evaporated by nitrogen steam at 40 °C. The result was resuspended in methanol (HPLC grade). Calibration curves were prepared by appropriate dilution of known volumes of the stock solution in methanol.

2.4. Preparation of DON solutions

DON concentration in the stock solution was checked by UV spectroscopy according to AOAC Official Methods of Analysis, Chapter 49 (AOAC, 2005), obtaining a concentration of the stock solution of 1336 μg/mL. Standard solutions of DON were prepared in methanol at a concentration of 10 μg/mL and stored at 4 °C. Calibration curves were prepared by appropriate dilution of known volumes of the stock solution with the mobile phase.

2.5. Ergosterol extraction in wheat

A total of 270 wheat samples were supplied by a feed producing agricultural cooperative. Their origin was Lleida province. They were taken within its quality control programme from each incoming truck. From the whole homogenized sample, a subsample (200-500 g) was sent to our laboratory. Concisely, 7 g of previously ground wheat with an IKA® A11 Basic mill (Darmstadt, Germany) were mixed with 40 mL of methanol and 10 mL of hexane. The mix was stirred 30 min at 112×g and filtered through a sieve of filter paper. 20 mL of the solution were transferred to a tube and 2 g of KOH were added. The tube was shaken with a magnetic stirrer and was placed into a bath at 55-60 °C for 20 min. The ergosterol extraction was performed adding, in a first step, 2 mL of bi-distilled water (to cool the solution) and 2 mL of hexane. The solution was stirred to enable a liquid-liquid extraction and the upper layer corresponding to the hexane phase was recovered. Two additional liquid-liquid extraction steps with 2 mL of hexane were performed, recovering a final extract volume from the three extractions of 6 mL. This volume was evaporated with low nitrogen steam at 40 °C. The dried samples were resuspended into 1 mL of methanol (HPLC grade) before being injected into the UHPLC-DAD system.

2.6. DON extraction in wheat

As stated before, the same samples were used for a mycotoxin analysis. DON was extracted using specific IAC columns (DONPREP®) following the manufacturer's instructions. The mycotoxin extraction followed a slightly modified version of the methodology used by Vidal, Sanchis, Ramos, & Marín (2018). Briefly, 7 g or 14 g, for the first and the second trial, respectively, previously ground with an IKA® A11 Basic mill (Darmstadt, Germany) were mixed with 42 and 78 mL, correspondingly, of MiliQ water in a 250 mL Erlenmeyer flask, followed by 10 min stirring. Then, samples were centrifuged for 10 min at 1780×g. Supernatant was filtered through a 9 mm of diameter glass microfiber filter paper (Whatman™ GF/A, Maidstone, UK) and 5 mL of the filtrate was passed through the IAC column. The column was then washed with 10 mL of bi-distilled water and the toxins were eluted with 3 mL of methanol HPLC-grade (the first 1.5 mL performing back-flushing). Samples were evaporated under a low nitrogen stream at 40 °C and resuspended in the mobile phase (methanol:acetonitrile:water, 5:5:90, v/v/v). Every resuspended extract was filtered through a nylon filter (0.4 μm) before being injected into the UHPLC-DAD system.

2.7. HPLC system for ergosterol analysis

The HPLC equipment consisted of a HPLC Waters 2695 system, with a Waters Spherisorb 5 μm ODS2, 4.6 × 250 mm analytical column coupled with a Waters 2487 UV/Visible dual λ absorbance detector set at 282 nm. The mobile phase was methanol (HPLC grade) at 1 mL min^{-1}, the injection volume was 100 μL and the total rum time was 18 min for each sample analysis. Ergosterol standard was purchased from Sigma (St. Louis, Mo) for calibration line (R^2 = 0.99). The limit of detection (LOD) of ergosterol in wheat was considered 0.5 mg/kg.

2.8. UHPLC system for DON analysis

The determination of DON was performed using an Agilent Technologies 1260 Infinity UHPLC system (California, USA) coupled with an Agilent 1260 Infinity II Diode Array Detector (DAD). A Gemini® C18 column from Phenomenex 150×4.6 mm (California, USA) with a

particle size of 5 μm and a pore size of 110 Å was used. Absorption wavelength was set at 220 nm. The mobile phase was composed of methanol:acetonitrile:water (5:5:90, v/v/v) and set at a flow rate of 1 mL min^{-1}. The column temperature was 40 °C, the injection volume was 50 μL and total run time was 15 min for mycotoxin analyses. The performance of the method for the quantification of DON in wheat was previously published in Vidal et al. (2018), in which the LOD was considered to be three times the signal of the blank (50 μg/kg).

2.9. Hyperspectral data processing for bulk ergosterol and DON determination

Firstly, the spectral data was obtained recording sample's mean reflectances for 167 wavelengths of 14 g from 50 samples as explanatory variables. A total of 150 images for unground samples and 150 images (50 samples in triplicate in both cases) for ground samples were obtained to develop a cross-validated model. The triplicates were achieved by shaking the samples between scans to randomly distribute the unground kernels or ground meal to obtain a major representativeness of the sample. The 14 g from each sample were divided into two subsamples of 7 g, one for ergosterol and the other for DON analysis. The ergosterol concentration range went from 1.9 to 18.7 mg/kg and DON contamination range included samples from <LOD to 2660.0 μg/kg. These results were obtained by HPLC and were categorized as the dependent variables.

Secondly, the prediction model was performed collecting sample's mean reflectances for 167 wavelengths of 14 g from 165 samples in the DON concentration range of <LOD - 2660.0 μg/kg as explanatory variables and DON concentration obtained by UHPLC as dependent variable. A total of 495 images (165 samples in triplicate) were obtained to develop a cross-validated model. The same samples were divided in two sets, in which kernels arising from 83 samples were scanned (249 images) for the calibration set and kernels from 82 samples (246 images) for the validation set.

Mean spectra were calculated from the pixel spectra of all scanned kernels. Triplicate spectra were treated independently to introduce a total of 495 observations in the multivariate analysis tool (The Unscrambler 7.6 SR1 software by CAMO AS, Oslo, Norway, 2001). On one hand, the

reflectances were transformed by a baseline correction to the absorbance spectra and, on the other hand, a first derivative application. A PLS model was built for each transformation and it was refined in order to simplify the model. Two prediction models were built. The first regression model used a full cross-validation to obtain the best RMSECV as possible. The second one used the two divided sample sets, in order to obtain the prediction performance with the RMSEP (Root Mean Square Error of Prediction). Some spectra were removed as they were considered outliers for the all the models. The criteria followed for outlier detection was to represent the influence plot, and reject those spectra with higher residual Y-variance, which described the mismatch between the sample and the model. The samples with high leverage and low residual Y-variance were considered extremal samples and they were maintained in the model. Sample with a high leverage and with high residual Y-variance were considered out of adjustment and with a reduced importance on the model, thus they were rejected. Less than 10% of the original spectra were removed. The criteria used to select the number of PCs to optimize the models (for cross-validation and for test set) was the PC number where the first minimum on the curve of the Root Mean Square Error (RMSE) occurs. Validation accuracy was assessed by the performance parameters, that is, the slope, correlation, coefficient of determination, RMSEP and Standard Error of Prediction (SEP).

The classification models were developed using the data from the preceding PLS model, that were 495 images from 165 samples at different concentrations. First, a cross-validated classification model was achieved. Moreover, the images were distributed into two sets, each of them covering the widest range of concentrations as possible for an independent validated model. Statistical analysis was performed with JMP PRO 14.1.0 (SAS Institute Inc., 2018) software using Linear Discriminant Analysis (LDA) model able to characterize two or more classes, first by a dimensionality reduction step and a second classification stage. The limit established for the two classes separation was the EU legal limit for DON (1250 µg/kg). From the 249 images used for the calibration and the 246 for the validation set, 411 corresponded to kernels arising from samples below 1250 µg/kg of DON and 84 to kernels from samples above

311 the legal limit. Accuracies were obtained as the percentage (%) of correctly classified images
312 from the total (495).

313 3. RESULTS

314 3.1. Ergosterol distribution in wheat samples

315 The mean concentration of the 50 samples was 6.13 mg/kg and the standard deviation was 3.64
316 mg/kg. The concentration range comprised samples from <0.5 mg/kg to 18.65 mg/kg. Finally,
317 the coefficient of variation (CV) obtained was 59.33 %. Fig. S1 (supplementary material)
318 represents the frequency of distribution of ergosterol concentration in the whole data set. The
319 highest frequencies are obtained for the medium-low concentrations (from 2 to 12 mg/kg), so
320 the distribution of the data is asymmetric under the mean.

321 3.2. Ergosterol quantification in wheat ground and unground samples through
322 HIS-NIR spectroscopy

323 PLS regression between Y variable (ergosterol HPLC results) and X variables (HSI-NIR
324 results) was performed for both whole and ground samples. The models were cross-validated as
325 they were calibrated with just 150 images. The performance results for raw spectra and both
326 spectral pretreatments are included in Table 1.

327 The application of 1st derivative on the raw spectra seemed to be the best pretreatment for wheat
328 unground samples, obtaining the lowest RMSEP (1.17 mg/kg) and the highest slope and
329 coefficient of determination (0.92 and 0.89, respectively) (Fig. 1). However, the model needed a
330 higher number of principal components (21) for its calibration. The models were debugged by
331 removing 14 outliers.

332 In the case of ground samples, 9 samples were considered as outliers. The results for the three
333 applied pretreatments are presented in Table 1. The best fitted model was the one built on the 1st
334 derivate spectra, in which the lowest RMSEP (1.57 mg/kg) was obtained and the slope and the
335 R^2 were higher than the obtained with other pretreatments (0.84 and 0.77, respectively) (Fig. 1).

Nevertheless, the principal components used in this model were also higher (23), so the model presented more complexity.

Based on these models, we considered to estimate DON concentration based on the ergosterol regression. To appraise the ability of ergosterol differences (independent variable, X) to explain DON variability (dependent variable, Y), a regression between both variables was performed (Fig. S2, supplementary material). It was carried out for 50 samples in which DON and ergosterol were previously analysed by HPLC. The coefficient of determination (R^2) of the adjustment was 0.37. This means that ergosterol could only explain a 37 % of the DON variation, thus it was concluded that ergosterol is not appropriate for indirect DON determination, even though it could determine the fungal growth. For that reason, a direct DON quantification by HSI-NIR is required.

3.3. DON variability in wheat samples

The distribution of DON concentration in the samples used in the present study for DON quantification and classification trials are reported in Fig. S3 (supplementary material). The statistics for the calibration and the validation sets are shown independently, with mean DON concentrations of 497.7 and 467.1 µg/kg, respectively. Both values are considered as low-contamination, due to the high frequency of samples above the LOD. Samples defined as high-contaminated contained maximum concentrations of 3537.0 and 2628.5 µg/kg for the calibration and the validation sets, respectively. Fig. S3 represents the frequency and the distribution of the reference DON content. The frequency histogram showed the number of samples in each category. A high-density of samples are located in the medium-low contaminated area of the representation which follows a non-Gaussian distribution, in which most of the DON contents are under the mean. This fact is expected to be due to the heterogeneity between batches in which fungal production of DON can depend on environmental factors, such as moisture, temperature or harvest season. The samples were divided with the aim to obtain two sets covering the widest range as possible and with similar

frequencies in all the levels of contamination for the calibration and validation. Fig. S3 shows that both sample groups showed similar distributions.

3.4. Quantification of DON in unground samples by HIS-NIR PLS regression

The models were based on 495 images (from 165 samples in triplicate) used for the calibration of the model. Different spectral pretreatments were introduced in order to find the best fitted model with the lowest error of prediction as possible so, apart from the raw data, a baseline correction to the absorbance spectra (ABS/BC) and a first derivative (1stD) were also tested. As the models were verified by cross-validation and for an independent test set (dividing the samples in two sets of 83 samples for calibration and 82 samples for validation), a total of six models were assembled for each data set. For both validations, the models were built using the same sample set. Their parameters are presented in Table 2.

From the original 495 images, a total of 23 (4.64 %) were rejected as outliers. The predicted versus measured plot and the performance parameters for the independent validation of best fitted model are shown in the Fig. 2. The trend line corresponds to the prediction regression line obtained for the validation of the model. The slope obtained was 0.59, the offset was 13.03 µg/kg, the correlation was 0.81, the coefficient of determination (R_v^2) was 0.61 and the root mean square error of prediction (RMSEP) was 501.36 µg/kg. The optimum number of PC used to fit the model were 13. From the spectral range used (895–1730 nm), two characteristic wavelengths contributed substantially to explain DON variance within the model. These spectral bands were a maximum peak at 1220 nm and a minimum at 1380 nm, whose regression coefficients had higher positive and negative weights than the rest of the wavelengths. Thus, both bands contributed significantly to the prediction of DON.

3.5. Classification of unground samples according to DON concentration by LDA

The 495 mean spectra from unground wheat samples used for the calibration of the models were introduced to the JMP Pro statistics software for a LDA classification. Two models were built,

one was validated by cross-validation and the other dividing the samples into training and validation sets. The classification threshold was established in the actual maximum EU limit (1250 µg/kg) for unprocessed cereals.

The results obtained for the cross-validated models are shown in the Table S1 (supplementary material). The use of 1st derivative spectra led the higher classification accuracies for LDA in which a 95.66 % of the samples were correctly classified. Only 24 samples were incorrectly classified, so it would be the best model for sample classification according to their DON level for a single data set. Otherwise, the classification accuracies achieved for the independent validation set were similar for the three pretreatments (Table 3). Despite of the similarity in the accuracies, the best accuracy was obtained for the 1st derivate pretreatment, in which 82.93 % of samples were correctly classified. Despite the similarity in the validation accuracies with other pretreatments, it was selected for its higher correctness in the training set (97.99), which provides robustness to the model. Consideration should be given to the significant number of samples with DON levels below the EU limit incorrectly classified as highly contaminated. It may be due to the elevate number of samples below the 1250 µg/kg (411) in comparison with the samples above the threshold in both calibration and validation sets.

3.6.Quantification of DON in ground samples by HIS-NIR PLS regression

The predictive model for ground samples was based on the regression of the same samples than in previous models. As for unground sample analysis, the same spectral pretreatments were applied to the raw data and validated in two ways, thus, six models were also built. The results obtained for all the models are collected in Table 4. The models with the best performance were obtained for the data transformed with the 1st derivative, which had the lower RMSEP and the higher R^2. The independent set validated model is represented by the measured versus predicted plots in the Fig. 3.

First, for the original 495 images used for the cross-validated model, 24 (4.84 %) were discarded as they were detected as outliers. These 471 samples were used to both calibrate and validate the model. The most remarkable performance parameters were a slope of 0.72, an offset

of 108.57 µg/kg, a correlation of 0.83, a coefficient of determination (R_{cv}^2) of 0.69 and a root mean square error of prediction (RMSEP) of 403.29 µg/kg. The model needed 16 PC to be correctly fitted.

Likewise, the same pretreatments were applied for ground samples spectra divided into a calibration and a test set. Only 5 (1.98 %) outliers were discarded from the calibration data as they were considered abnormal compared with the major part of the data. The regression parameters were a slope of 0.55, an offset of 122.30 µg/kg, a correlation of 0.78, a coefficient of determination (R^2) of 0.59 and a root mean square error of prediction (RMSEP) of 518.95 µg/kg. The predictive model needed a smaller number of PC than for its cross-validated obtaining an optimum number of PC of 10. In this case, two wavelengths were also detected to highly contribute to explain the variance of DON into the model. However, these two wavelengths were positioned at the spectral extremes (941.7 and 1728 nm), where for the 1st derivate spectra noise is enhanced (Agelet & Hurburgh, 2010). A third wavelength (1380 nm) also had a significant weight on the model (local minimum), which matched with the characteristic wavelengths found in the models for unground wheat. This fact led us to select unground samples as a more reliable choice for model development.

3.7. Classification of ground samples according to DON concentration by LDA

A total of 495 images were used for they classification by LDA. Initially, all the images were used for the estimation of the classification performance by a cross-validation. Then, they were divided into a training and a validation set for an independent validation. The process used to obtain ground samples consisted only in a milling step, in which the product obtained was not refined, so the wheat bran was maintained in the samples. Thus, the classification threshold was established at the UE maximum limit of DON (1250 µg/kg), as for unprocessed cereals.

The first model results are collected in the Table S2. As for the unground sample analysis, the 1st derivative pretreated spectra presented the highest classification accuracy (97.18 %), beyond the non-treated and the absorbance and baseline corrected spectra results (94.35 and 84.05 %, respectively). An important consideration should be given to the low number of over-limit

442 samples misclassified as under-limit contaminated samples in all cases. For the 1st derivative
443 model a single high-contaminated sample was classified under the limit. Conversely, the LDA
444 results for the training and validation sets are gathered in the Table 5. The highest accuracy for
445 the training set was obtained for the 1st derivate spectra with 99.20 %. In addition, the
446 accuracies obtained for the validation set were similar for both absorbance and baseline
447 corrected spectra and for 1st derivate spectra (87.81 and 85.37 %, respectively), although the 1st
448 derivative model presented a higher overall accuracy. For the absorbance transformed and
449 baseline corrected spectra, the calibration efficiency was poorer than in the validation step. This
450 could occur as the validation was done with a different sample set not used in calibration.
451 Nevertheless, the accuracies of the 1st derivative corrected spectra as a whole (training and
452 validation) presented higher overall performances than the ABS/BC transformed data set
453 efficiencies. As in the cross-validated models, few samples with concentrations over the limit
454 were misclassified as under-limit.

455 ## 4. DISCUSSION

456 ### 4.1. Ergosterol quantification in wheat samples through HIS-NIR spectroscopy

457 Ergosterol was detected in all wheat samples, with most of the samples showing medium-low
458 content, while few samples presented high concentrations. This suggests that all samples
459 presented fungal contamination. Our ergosterol results presented higher contents than
460 Perkowski et al. (2008) who presented a range of 0.40-3.40 mg/kg for naturally-infected wheat
461 and similar results to Lamper et al. (2000) with a range from 1.46 to 42.14 mg/kg. This
462 demonstrated that our samples covered a wider range of concentrations than others naturally-
463 infected, making them appropriate for HSI-NIR evaluation.

464 In the present work, the quantitative correlation between fungal growth, in terms of ergosterol
465 content, and DON incidence in wheat was assessed. A weak correlation of 0.63 between
466 ergosterol and DON concentrations was observed. Comparing our study with that of Barbedo et
467 al. (2015), in which they tried to establish a correlation between a *Fusarium* Index (based on
468 visual symptoms) and DON, they obtained a correlation of 0.84, which is higher than ours. Both

visual symptoms and ergosterol content are indirect indicators of fungal growth which may be representing different stages of fungal growth, thus none of them are perfect. Furthermore, ergosterol content accounts for fungal presence and not exclusively for DON-producing *Fusarium* incidence, so we are obtaining an estimation of fungal growth on wheat, although it can be due to other species. Moreover, ergosterol could be produced in wheat before DON production, thus the correlation between fungal growth and this compound is not perfect.

In our previous study (Femenias et al., 2020) we assessed the correlation between kernel symptomatology and DON contamination using PCA, which showed that, in general, DON contaminated kernels showed visible symptoms, but could also occur in asymptomatic kernels. Nevertheless, the kernels used to build the PCA were not individually analysed, but the contamination was evaluated from the whole sample, so it must be taken in consideration. Paul, Lipps, & Madden (2005) study evaluates the relationship between visual *Fusarium* Damaged Kernels (FDK) assessment and DON, in which they also obtained an imperfect correlation of 0.73. Moreover, Stanisz, Zgola-Grezeskowiak, Stepien, & Beszterda (2015) obtained a weaker R^2 (0.068) between ergosterol and DON concentration in wheat samples. Even though the ergosterol is found in higher concentrations than DON and it would be a great compound for indirect DON detection, the correlation between both substances is insufficient for accurate mycotoxin detection. In addition, to build a DON predictive analysis from wheat ergosterol content by HSI-NIR, the predictive deviation of its adjustment should be added to the weak ability of ergosterol to predict DON ($R^2 = 0.37$), thus the indirect detection would present higher disadvantages in comparison with a direct model calibration of DON by HSI-NIR.

Interestingly, the HIS-NIR models from unground samples performed better than those for ground samples. This fact could be attributed to the fact that ergosterol is expected to be present in the surface of the kernels as a result of fungi colonising their surface, thus grounding would led to a reduced detection of ergosterol. The high-influence coefficients of regression were extracted for the best fitted model. Two maxima (983.8 and 1701 nm) and two minima (960.3 and 1380 nm) peaks are considered to have the highest weights on the model, which would

explain ergosterol variability. One of the first publications that quantified ergosterol in wheat samples by NIR was from Dowell et al. (1999) who adjusted their model with a R^2 of 0.62 and a SEC of 108 mg/kg for ergosterol concentrations above 50 mg/kg. As in our study, they used all the spectral range that was comprised between 500-1700 nm. These results were improved by recent reports (Berardo et al., 2005; Börjesson et al., 2007) that worked with maize and barley, respectively. Berardo et al. (2005) best regression models showed a R^2 of 0.81 and a SEP of 1.74 mg/kg using characteristics bands of 1430, 1470, 1820, 2140, and 2180 nm and Börjesson et al. (2007) detected ergosterol by NIR reflectance with a R^2 of 0.83 and a RMSE of 4.5 mg/kg, considering the whole complex information from the NIR region to estimate ergosterol. Our best results (1^{st} derivate spectra for unground kernels) showed lower errors (RMSEP = 1.17 mg/kg) and higher R^2 (0.89). In our study, four wavelengths (960, 983.8, 1380 and 1701 nm) presented higher weights on the whole model as they explained much variance of ergosterol than other bands. Only the 1400 nm region of the spectra was also used in previous studies for ergosterol detection. Furthermore, HIS-NIR spectroscopy may be more appropriate to describe ergosterol content by the reflectance of the surface of unground wheat kernels, due to our results for ground samples presented weaker adjustment parameters (R^2 of 0.77) than previous reports. In conclusion, HIS-NIR spectroscopy would be a suitable method to assess grain quality in terms of fungal presence, but not to assess wheat safety in terms of DON.

4.2. DON quantification in wheat samples through HIS-NIR

From the 165 original samples analysed by the reference method, 62 presented concentrations under the LOD. Ideally, the data set should represent the widest DON concentration range as possible which represents the maximum variability to build a solid prediction model. Our results presented a distribution of DON which showed a high density of samples in low concentrations. Despite this, the key point of this study is that it was carried out with naturally-contaminated samples, and consequently, results are directly applicable in real situations for DON prediction in wheat. In addition, the data set was equally divided into calibration and validation groups, covering similar ranges of concentration. Balanced sets of data are required to obtain validation

performance parameters that represent the maximum variance of the model calibration. The models were performed for unground and ground wheat samples for which 1st derivative was the best pretreatment for both. For the intact grain, a slope of 0.59, a R^2 of 0.61 and a RMSEP of 501 µg/kg were obtained. For the milled, a slope of 0.55, a R^2 of 0.59 and a RMSEP of 518 µg/kg were achieved. These results provide slightly higher performances for unground samples than for ground. Avoiding the grinding step presents advantages to the method, which would be faster and the complexity of the method is reduced.

Preliminary studies used pre-HSI technology for DON quantification, in which the majority are based on NIR, Fourier Transformed NIR (FT-NIR) and Middle Infrared (MIR). Although these technologies are not able to recognize the spatial distribution of the cereals, first approximations were developed for mycotoxin content prediction by Peiris, Pumphrey, & Dowell (2009). In their study, they mentioned the typical absorption wavelengths of DON, which were 1408 nm, 1904 and 1919 nm for the second derivative spectra. To reach their results, they worked with pure DON diluted into acetonitrile to scan it by NIR, consequently the results are not entirely comparable as they worked with a different matrix. Although the spectral range used in our study do not cover the same spectral range (maximum 1728 nm), our characteristic wavelength (1380 nm) is close to the 1408 nm band reported in the mentioned study. In our research, the extracted 1380 nm band was highly explanatory in both ergosterol and DON models. This led us to consider that DON producing fungi presence could be explained by the abovementioned NIR region.

Dvořáček, Prohasková, Chrpová, & Štočková (2012) estimated DON content in intact wheat samples by FT-NIR, thus we can discuss their results with our outcomes for unground wheat. Their best PLS-DA result showed a high correlation of 0.92, but also a high SEP of 2.35 mg/kg. Unlike in our study, they used ELISA as reference method and they worked on artificially contaminated samples at a higher DON range (0-90 mg/kg). Moreover, they identified two spectral regions between 1390-1770 nm and 1880-2070 nm which would describe DON contamination. Our methodology is focused on the NIR spectra, which goes from 895 nm to

1728 nm, thus only the first region could be compared to our results. Conversely, Jin et al. (2014) obtained a R^2 of 0.46 for NIR analysed wheat inoculated single kernels with a DON contamination range from 0.46 to 29.25 mg/kg. Different reference methods from our study were used (GC-MS and visual inspection). In the same way we proceeded in our study, they used the whole spectra for the calibration of the model. Additionally, the study of Peiris, Dong, Davis, Bockus, & Dowell (2017) obtained a SEP of 2400 µg/kg and an R^2 of 0.48, and, in this case, the whole spectral range with a mean centering was used for the calibration process. They scanned 65-70 g of non-milled wheat, thus their model parameters can be compared to ours for unground samples. However, some spectral bands were related to the presence of DON, as they correlated them with the bonds vibrations of the DON molecule. They found spectral peaks in their regression coefficients at 1310, 1400, 1420, 1920 and 1960 nm. The first three could be compared to our peak at the same spectral region (1380 nm) which led us consider it as the region of maximum information for DON. It is remarkable that the present study is the first one in which naturally contaminated wheat samples were used for HSI-NIR technology.

HSI-NIR technologies have been used by few authors for DON quantification. Although the study was performed with oat single unground kernels, Tekle, Mage, Segtnan, & Bjornstad (2015) used HSI-NIR for a rapid DON estimation. The PLS performance cannot be fully compared with our results, as they used a cubic logarithm of DON concentration as dependent variable for oat single grain. However, an optimal correlation of 0.81 was achieved. Only one of the peaks which permitted the DON detection were comparable to our spectral range, which was the 1400 nm wavelength. In this case, it is also very close to the band which explained more of the information in our model (1380 nm). In our previous study (Femenias et al., 2020), the PLS regression parameters for bulk samples were poorer than in the present one, although the number of samples in the present study have been increased, and exactly the same kernels from each sample were used for both analysis. The R^2 has increased from 0.27 to 0.61 and the RMSEP has been reduced from 1174 µg/kg to 501 µg/kg. Moreover, the 1st derivative of the spectra, which was not established as the best spectral pretreatment method for DON-

577 contaminated single kernel discrimination by PCA in our previous work, presents the best
578 results for bulk kernel analysis by PLS regression in the present work. However, comparing the
579 absorbance and baseline corrected spectra model results from both studies, the PLS parameters
580 have also improved (R^2 of 0.52 and RMSEP of 561 µg/kg). The characteristic peaks obtained in
581 the previous study were local minima or maxima in 955 nm, 1287, 1403, 1455, 1528, 1671 and
582 1714 nm. The pretreatment of the spectral data may introduce changes in our spectral behaviour,
583 but our peaks are still comparable to the ones obtained in unground models previously presented
584 (1220 and 1380 nm). However, the selection of the unground model for DON determination
585 would avoid characteristic bands near the extremes which introduce noise to the ground wheat
586 model (Agelet & Hurburgh, 2010; Yao & Lewis, 2010).

587 Our results can be compared with De Girolamo, Lippolis, Nordkvist, & Visconti (2009)
588 outcomes, who also worked with ground naturally-contaminated wheat samples and with a
589 similar concentration range (50-3000 µg/kg), but they used FT-NIR to scan milled and sieved
590 wheat. For our ground model, we obtained a similar slope and coefficient of determination for
591 the cross-validated model (0.72 and 0.69, respectively) than in their case (0.71 in both cases).
592 Nevertheless, our RMSECV was better (403 µg/kg) than the one obtained in the previous study
593 (516 µg/kg). For the independent validation of the model of milled samples, the R^2 was slightly
594 lower (0.59) than the compared study (0.63) and the RMSEP was better (518 µg/kg) than the
595 868 µg/kg obtained by De Girolamo et al. (2009). Moreover, the high-influence peaks of this
596 study were situated at 1409 nm region and at the 1904 nm band. Our results pointed out also to
597 the spectral region near the 1400 nm, which may be related to DON contamination. In addition,
598 De Girolamo, Cervellieri, Visconti, & Pascale (2014) used FT-NIR for DON evaluation in
599 ground naturally-contaminated wheat samples. In this case, the range of concentration raised up
600 to 16,000 µg/kg. First, PLS results for ground and sieved samples presented a reduced
601 prediction capacity in comparison with our model (only ground). They obtained a RMSEP of
602 1,977 µg/kg and an R^2 of 0.63. Although their coefficient of determination was similar to ours
603 (0.69), their RMSEP was much higher than ours (403 µg/kg). This increase in the RMSEP could

be attributed to the raised up DON range, which depends on the original Y variable scale. In the last two studies, both sieved their samples with a sample size < 500 µm. This step may reduce sample heterogeneity at the expense of losing DON, which is found with higher probability at the external layer of the kernel. Thus, during the milling step, the larger particles corresponded to the outer layer while the small particles to the endosperm. To avoid DON loss in our samples, we avoided the sieving step, which also introduces time consume and complexity to the analysis.

4.3. Classification of wheat samples according to DON levels through HSI-NIR

Peiris et al. (2010) published one of the first studies focused on wheat sorting according to kernel DON levels by NIR spectroscopy. The methodology used is not fully comparable with ours, as they worked with single kernel analysis and they had a high concentration range. However, they achieved a classification accuracy of 96 % fixing the threshold in 60 mg/kg. Despite of the high accuracy obtained, the cut-off established was too high to be applied to contaminated batches at industrial level.

As in the present study, De Girolamo et al. (2014, 2009) also classified milled wheat samples by LDA. In the first study, they obtained an accurate precision of 69% of correctly classified samples with a DON contamination cut-off in 300 µg/kg. A high precision accuracy from 75-90% was achieved for 3 classes discrimination (< 1000 µg/kg; 1000-2500 µg/kg; > 2500 µg/kg) by De Girolamo et al. (2014) using FT-NIR, which is comparable to our results of more than a 82% of correctly classified samples. Despite of the high-accuracy of classification obtained, from the 495 spectra used in this work, only 84 corresponded to samples above the UE maximum limit. Future studies should evaluate the introduction of similar frequencies of DON between groups above and under the threshold to have the same weight in the model.

Peiris et al. (2017) also employed the FT-NIR device for DON classification in different thresholds. The spectral range was comprised between the non-detectable levels to 58,100 µg/kg. Their closest cut-off to the one used in this work was 2000 µg/kg. Their overall classification accuracy for this cut-off was 87%, similar to ours. Nevertheless, their

631 classification accuracy for the samples below the threshold (only a 7.2% of the total samples)
632 was 38.9%. In our case, we used a higher number of samples below the limit with 96 % of
633 correctly classified samples. This demonstrated that it may be possible to manage naturally
634 contaminated wheat batches in which these moderate concentrations are frequently found.
635 However, we need a more balanced data set in which high-contaminated samples are found in
636 similar frequencies than low-contaminated ones.

637 Moreover, Barbedo et al. (2017) published the first study which tried to evaluate DON by HSI
638 in the NIR region. Despite they did not consider feasible the estimation of DON content, they
639 focused in a classification method of wheat batches in two or three categories. The two
640 categories model followed the EU legal limit for unprocessed cereals (1250 µg/kg) as the cut-
641 off. They achieved a correctly sorting ratio of 81% for two groups splitting which is slightly
642 lower than ours (83%). Our study presented differences in the sampling conditions, in which the
643 sample consisted in 14 g (approximately 400 kernels), different to their 30-50 kernels in each
644 image. Consequently, our sample volume would be more representative of the whole batch for
645 future classifications, in which more spectral features can be represented.

646 A more statistically complex research has been published by Liang et al. (2018) in which
647 spectral preprocessings and novel algorithms were assembled for the determination of different
648 DON levels in wheat bulk samples. The classes were divided into three mean levels of < 250,
649 1162 and 2665 µg/kg for a PLS-DA classification. Samples containing from 250 to 5000 µg/kg
650 were analysed by HSI-Vis/NIR. The wavelength range was between 250-1000 nm, so that only
651 one peak (980 nm) can be compared with our spectra (893-1731 nm). Consequently, their
652 characteristic wavelengths cannot be compared with the present study, as they worked in a
653 different spectral range. Even though the computation of their models was complex, they
654 obtained high classification accuracies achieving their best result for the MSC-SPA-SVM
655 combination, which obtained a 97.75% of correctly classified samples for the test set.

5. CONCLUSIONS

Food and feed industries have an urgent need for rapid methods which allow analysis and rejection of mycotoxin contaminated batches in a short period of time. Traditional screening analysis, such as ELISA and LFD, could be replaced by rapid and non-destructive screening methods with the application of HSI-NIR technique for fungal growth and DON inspection. It has been demonstrated that in spite of the low correlation between ergosterol and DON, successful outcomes of ergosterol quantification with high performance could be achieved by HSI-NIR. In addition, the findings established that it could be possible to quantify DON in bulk naturally contaminated wheat samples with a 501.36 µg/kg error of prediction. With such error this quantification could be used as a screening tool. However, the classification model used to reject samples according to the UE maximum limit presented remarkable accuracies (> 90%), which could be applied to discard high-contaminated batches entering in food chain. In addition to the foregoing, further studies including single kernel screening will be required to avoid the whole batch discard by individual kernel sorting to improve DON reduction and production yield.

6. CONFLICTS OF INTEREST

The authors declare that they have no conflict of interest.

7. AKNOWLEDGEMENTS

The authors are grateful to the University of Lleida (predoctoral grant), and to the Spanish Ministry of Science, Innovation and Universities (Project AGL2017-87755-R) for funding this work.

8. BIBLIOGRAPHY

Agelet, L. E., & Hurburgh, C. R. (2010). A tutorial on near infrared spectroscopy and its calibration. *Critical Reviews in Analytical Chemistry*, *40*(4), 246–260. https://doi.org/10.1080/10408347.2010.515468

Alisaac, E., Behmann, J., Rathgeb, A., Karlovsky, P., Dehne, H. W., & Mahlein, A. K. (2019). Assessment of *Fusarium* infection and mycotoxin contamination of wheat kernels and flour using hyperspectral imaging. *Toxins*, *11*(10), 1–18. https://doi.org/10.3390/toxins11100556

AOAC. (2005). Official Methods of Analysis. *Official Methods of Analysis of AOAC International*, *18*, 20877–22417.

Barbedo, J. G. A., Tibola, C. S., & Fernandes, J. M. C. (2015). Detecting Fusarium head blight in wheat kernels using hyperspectral imaging. *Biosystems Engineering*, *131*, 65–76. https://doi.org/10.1016/j.biosystemseng.2015.01.003

Barbedo, J. G. A., Tibola, C. S., & Lima, M. I. P. (2017). Deoxynivalenol screening in wheat kernels using hyperspectral imaging. *Biosystems Engineering*, *155*, 24–32. https://doi.org/10.1016/j.biosystemseng.2016.12.004

Berardo, N., Pisacane, V., Battilani, P., Scandolara, A., Pietri, A., & Marocco, A. (2005). Rapid detection of kernel rots and mycotoxins in maize by near-infrared reflectance spectroscopy. *Journal of Agricultural and Food Chemistry*, *53*(21), 8128–8134. https://doi.org/10.1021/jf0512297

Beyer, M., Pogoda, F., Ronellen, F. K., Hoffmann, L., & Udelhoven, T. (2010). Estimating deoxynivalenol contents of wheat samples containing different levels of *Fusarium*-damaged kernels by diffuse reflectance spectrometry and partial least square regression. *International Journal of Food Microbiology*, *142*, 370–374. https://doi.org/10.1016/j.ijfoodmicro.2010.07.016

Boldrini, B., Kessler, W., Rebnera, K., & Kessler, R. W. (2012). Hyperspectral imaging: A review of best practice, performance and pitfalls for in-line and on-line applications. *Journal of Near Infrared Spectroscopy*, *20*(5), 483–508. https://doi.org/10.1255/1003

Börjesson, T., Stenberg, B., & Schnürer, J. (2007). Near-infrared spectroscopy for estimation of ergosterol content in barley: A comparison between reflectance and transmittance

techniques. *Cereal Chemistry*, *84*(3), 231–236. https://doi.org/10.1094/CCHEM-84-3-0231

Caporaso, N., Whitworth, M. B., & Fisk, I. D. (2018). Near-Infrared spectroscopy and hyperspectral imaging for non-destructive quality assessment of cereal grains. *Applied Spectroscopy Reviews*, *53*(8), 667–687. https://doi.org/10.1080/05704928.2018.1425214

De Girolamo, A., Cervellieri, S., Visconti, A., & Pascale, M. (2014). Rapid analysis of deoxynivalenol in durum wheat by FT-NIR spectroscopy. *Toxins*, *6*(11), 3129–3143. https://doi.org/10.3390/toxins6113129

De Girolamo, A., Lippolis, V., Nordkvist, E., & Visconti, A. (2009). Rapid and non-invasive analysis of deoxynivalenol in durum and common wheat by Fourier-Transform Near Infrared (FT-NIR) spectroscopy. *Food Additives & Contaminants: Part A*, *26*(6), 907–917. https://doi.org/10.1080/02652030902788946

Delwiche, S. R., Kim, M. S., & Dong, Y. (2011). *Fusarium* damage assessment in wheat kernels by Vis/NIR hyperspectral imaging. *Sensing and Instrumentation for Food Quality and Safety*, *5*(2), 63–71. https://doi.org/10.1007/s11694-011-9112-x

Delwiche, S. R., Rodriguez, I. T., Rausch, S. R., & Graybosch, R. A. (2019). Estimating percentages of *Fusarium*-damaged kernels in hard wheat by near-infrared hyperspectral imaging. *Journal of Cereal Science*, *87*, 18–24. https://doi.org/10.1016/j.jcs.2019.02.008

Dowell, F. E., Ram, M. S., & Seitz, L. M. (1999). Predicting scab, vomitoxin, and ergosterol in single wheat kernels using near-infrared spectroscopy. *Cereal Chemistry*, *76*(4), 573–576. https://doi.org/10.1094/CCHEM.1999.76.4.573

Dvořáček, V., Prohasková, A., Chrpová, J., & Štočková, L. (2012). Near infrared spectroscopy for deoxynivalenol content estimation in intact wheat grain. *Plant, Soil and Environment*, *58*(4), 196–203. https://doi.org/10.17221/684/2011-PSE

Esbensen, K. H., Swarbrick, B., Westad, F., Whitcombe, P., & Anderson, M. J. (2018). *Multivariate Data Analysis: An introduction to Multivariate Analysis, Process Analytical*

Technology and Quality by Design. (CAMO, Ed.) (6th ed.).

Femenias, A., Gatius, F., Ramos, A. J., Sanchis, V., & Marín, S. (2020). Standardisation of near infrared hyperspectral imaging for quantification and classification of DON contaminated wheat samples, *111*(May 2020), 107074. https://doi.org/10.1016/j.foodcont.2019.107074

Fox, G., & Manley, M. (2014). Applications of single kernel conventional and hyperspectral imaging near infrared spectroscopy in cereals. *Journal of the Science of Food and Agriculture*, *94*(2), 174–179. https://doi.org/10.1002/jsfa.6367

Jin, F., Bai, G., Zhang, D., Dong, Y., Ma, L., Bockus, W., & Dowell, F. (2014). *Fusarium*-damaged kernels and deoxynivalenol in *Fusarium*-infected U.S. winter wheat. *Phytopathology*, *104*(9), 472–478. https://doi.org/https://doi.org/10.1094/PHYTO-07-13-0187-R

Lamper, C., Téren, J., Bartók, T., Komorowski, R., Mesterházy, Á., & Sági, F. (2000). Predicting DON contamination in *Fusarium*-infected wheat grains via determination of the ergosterol content. *Cereal Reserach Communications*, *28*(3), 2000. https://doi.org/10.1007/BF03543613

Liang, K., Liu, Q. X., Xu, J. H., Wang, Y. Q., Okinda, C. S., & Shena, M. X. (2018). Determination and visualization of different levels of deoxynivalenol in bulk wheat kernels by hyperspectral imaging. *Journal of Applied Spectroscopy*, *85*(5), 953–961. https://doi.org/10.1007/s10812-018-0745-y

Magan, N. (1993). Early detection of fungi in stored grain. *International Biodeterioration and Biodegradation*, *32*(1–3), 145–160. https://doi.org/10.1016/0964-8305(93)90047-6

Mancinelli, G., Costantini, M. L., & Rossi, L. (2014). Predicting ergosterol in leaf litter by near-infrared spectroradiometry: A preliminary assessment. *European Journal of Soil Biology*, *63*, 49–54. https://doi.org/10.1016/j.ejsobi.2014.05.003

Pandey, P., Srivastava, S., & Mishra, H. N. (2018). Comparison of FT-NIR and NIR for evaluation of phyisco-chemical properties of stored wheat grains. *Food Quality and Safety*,

759 *2*(3), 165–172. https://doi.org/10.1093/fqsafe/fyy015

760 Paul, P. A., Lipps, P. E., & Madden, L. V. (2005). Relationship between visual estimates of
761 Fusarium Head Blight intensity and deoxynivalenol accumulation in harvested wheat
762 grain: A meta-analysis. *Phytopathology*, *95*(10), 1225–1236.
763 https://doi.org/10.1094/PHYTO-95-1225

764 Peiris, K. H. S., Dong, Y., Davis, M. A., Bockus, W. W., & Dowell, F. E. (2017). Estimation of
765 the deoxynivalenol and moisture contents of bulk wheat grain samples by FT-NIR
766 spectroscopy. *Cereal Chemistry Journal*, *94*(4), 677–682.
767 https://doi.org/10.1094/CCHEM-11-16-0271-R

768 Peiris, K. H. S., Pumphrey, M. O., Dong, Y., Maghirang, E. B., Berzonsky, W., & Dowell, F. E.
769 (2010). Near-infrared spectroscopic method for identification of Fusarium head blight
770 damage and prediction of deoxynivalenol in single wheat kernels. *Cereal Chemistry*,
771 *87*(6), 511–517. https://doi.org/10.1094/CCHEM-01-10-0006

772 Peiris, K. H. S., Pumphrey, M. O., & Dowell, F. E. (2009). NIR Absorbance characteristics of
773 deoxynivalenol and of sound and *Fusarium*-damaged wheat kernels. *Journal of Near*
774 *Infrared Spectroscopy*, *17*(4), 213–221. https://doi.org/10.1255/jnirs.846

775 Perkowski, J., Bu, M., Stuper, K., Kostecki, M., Matysiak, A., & Szwajkowska-michalek, L.
776 (2008). Concentration of ergosterol in small-grained naturally contaminated and
777 inoculated cereals. *Biologia*, *63*(4), 542–547. https://doi.org/10.2478/s11756-008-0083-2

778 Pestka, J. J. (2010). Deoxynivalenol: Mechanisms of action, human exposure, and toxicological
779 relevance. *Archives of Toxicology*, *84*(9), 663–679. https://doi.org/10.1007/s00204-010-
780 0579-8

781 Ropelewska, E., & Zapotoczny, P. (2018). Classification of *Fusarium*-infected and healthy
782 wheat kernels based on features from hyperspectral images and flatbed scanner images: a
783 comparative analysis. *European Food Research and Technology*, *244*(8), 1453–1462.
784 https://doi.org/10.1007/s00217-018-3059-7

785 Seitz, L. M. (1979). Ergosterol as a measure of fungal growth. *Phytopathology*, *69*(11), 1202.
786 https://doi.org/10.1094/phyto-69-1202

787 Serranti, S., Cesare, D., & Bonifazi, G. (2013). The development of a hyperspectral imaging
788 method for the detection of *Fusarium*-damaged, yellow berry and vitreous Italian durum
789 wheat kernels. *Biosystems Engineering*, *115*(1), 20–30.
790 https://doi.org/10.1016/j.biosystemseng.2013.01.011

791 Stanisz, E., Zgola-Grezeskowiak, A., Stepien, L., & Beszterda, M. (2015). Can ergosterol be an
792 indicator of *Fusarium* fungi and mycotoxins in cereals products? *Journal of Braz. Chem.*
793 *Soc.*, *26*(4), 705–712. https://doi.org/http://dx.doi.org/10.5935/0103-5053.20150030 J.

794 Tekle, S., Mage, I., Segtnan, V. H., & Bjornstad, A. (2015). Near-infrared hyperspectral
795 imaging of *Fusarium*-damaged oats (*Avena sativa* L.). *Cereal Chemistry*, *92*(1), 73–80.
796 https://doi.org/10.1094/CCHEM-04-14-0074-R

797 Vidal, A., Sanchis, V., Ramos, A. J., & Marín, S. (2018). Stability of DON and DON-3-
798 glucoside during baking as affected by the presence of food additives. *Food Additives and*
799 *Contaminants - Part A Chemistry, Analysis, Control, Exposure and Risk Assessment*,
800 *35*(3), 529–537. https://doi.org/10.1080/19440049.2017.1401741

801 Yao, H., & Lewis, D. (2010). *Chapter 2. Spectral Preprocessing and Calibration Techniques*.
802 In: Hyperspectral Imaging for Food Quality Analysis and Control. Sun, D-W. (Ed.).
803 Academic Press, San Diego, CA, USA. https://doi.org/10.1016/B978-0-12-374753-
804 2.10002-4

805

806 **Figure captions**

807 Figure 1. Predicted vs. measured plot of ergosterol PLS regression for 1st derivate spectra. a)
808 Unground wheat data set. Optimum number of PC = 21; N = 135. b) Ground wheat data set.
809 Optimum number of PC = 21; N = 141.

Figure 2. Predicted vs. measured plot for the PLS validation set in unground samples. Optimum number of PC = 13. N of validation = 239.

Figure 3. Predicted vs. measured plot for PLS validation set. Optimum number of PC = 10. N of validation = 243.

Table 1. Performance parameters of ergosterol predictive models.

Sample	**Pretreatment**	**Slope**	**RMSEP (mg/kg)**	**R^2**	**Number of PC**
Whole samples	Raw spectra	0.88	1.35	0.85	20
	ABS/BC	0.85	1.35	0.82	18
	1^{st} derivative	0.92	1.17	0.89	21
Ground samples	Raw spectra	0.62	2.15	0.57	10
	ABS/BC	0.60	2.24	0.53	11
	1^{st} derivative	0.84	1.57	0.77	23

ABS/BC = Baseline-corrected absorbance spectra; PC = Principal Components; RMSEP = Root Mean Square Error of Prediction; R^2 = Coefficient of Determination.

824 Table 2. Performance parameters of DON predictive models for unground samples.

Bulk samples	Validation	Slope	RMSEP (µg/kg)	R^2	Number of PC
Raw spectra	Cross-validation	0.67	252.70	0.62	18
ABS/BC	Cross-validation	0.59	503.76	0.55	20
1st derivative	Cross-validation	0.76	354.28	0.73	16
Raw spectra	Test set validation	0.56	540.19	0.56	15
ABS/BC	Test set validation	0.58	561.04	0.52	14
1st derivative	Test set validation	0.59	501.36	0.61	13

825 ABS/BC = Baseline-corrected absorbance spectra; PC = Principal Components; RMSEP = Root
826 Mean Square Error of Prediction; R^2 = Coefficient of Determination.

827

828

829

830

831

832

833

834

835

836

Table 3. Linear discriminant analysis (LDA) accuracies for training and validation sets in unground samples.

	Training set				Validation set			
		Predicted		Accuracy (%)		Predicted		Accuracy (%)
Raw spectra	Groups	B	C	86.35	Groups	B	C	82.52
	B	170	34		B	172	35	
	C	0	45		C	8	31	
ABS/BC	Groups	B	C	86.35	Groups	B	C	83.33
	B	172	32		B	174	33	
	C	2	43		C	8	31	
1st Derivative	Groups	B	C	97.99	Groups	B	C	82.93
	B	199	5		B	170	37	
	C	0	45		C	5	34	

B = low-contaminated group of samples (< 1250 µg/kg); C = contaminated group of samples (> 1250 µg/kg). Grey cells indicate the number of correctly-classified samples. White cells indicate the number of miss-classified samples.

852 Table 4. Performance parameters of DON predictive models for ground samples.

Bulk samples	Validation	Slope	RMSEP (ppb)	R^2	Number of PC
Raw spectra	Cross-validation	0.72	483.28	0.62	13
ABS/BC	Cross-validation	0.73	438.94	0.70	16
1st derivative	Cross-validation	0.72	403.29	0.69	16
Raw spectra	Test set validation	0.55	578.68	0.49	7
ABS/BC	Test set validation	0.71	588.21	0.48	13
1st derivative	Test set validation	0.55	518.95	0.59	10

853 ABS/BC = Baseline-corrected absorbance spectra; PC = Principal Components; RMSEP = Root
854 Mean Square Error of Prediction; R^2 = Coefficient of Determination.

855

856

857

858

859

860

861

862

863

864

865 Table 5. Linear discriminant analysis (LDA) accuracies for training and validation sets

866 (threshold 1250 µg/kg) in ground samples.

	Training set				Validation set			
		Predicted		Accuracy		Predicted		Accuracy
Raw spectra	Groups	B	C	93.58	Groups	B	C	82.53
	B	191	13		B	176	31	
	C	3	42		C	12	27	
ABS/BC	Groups	B	C	83.14	Groups	B	C	87.81
	B	168	36		B	180	27	
	C	6	39		C	3	36	
1st Derivative	Groups	B	C	99.2	Groups	B	C	85.37
	B	203	1		B	188	19	
	C	1	44		C	7	22	

867 B = low-contaminated group of samples (< 1250 µg/kg); C = contaminated group of samples (>

868 1250 µg/kg). Grey cells indicate the number of correctly-classified samples. White cells indicate

869 the number of miss-classified samples.

870

Figure 1

Click here to download high resolution image

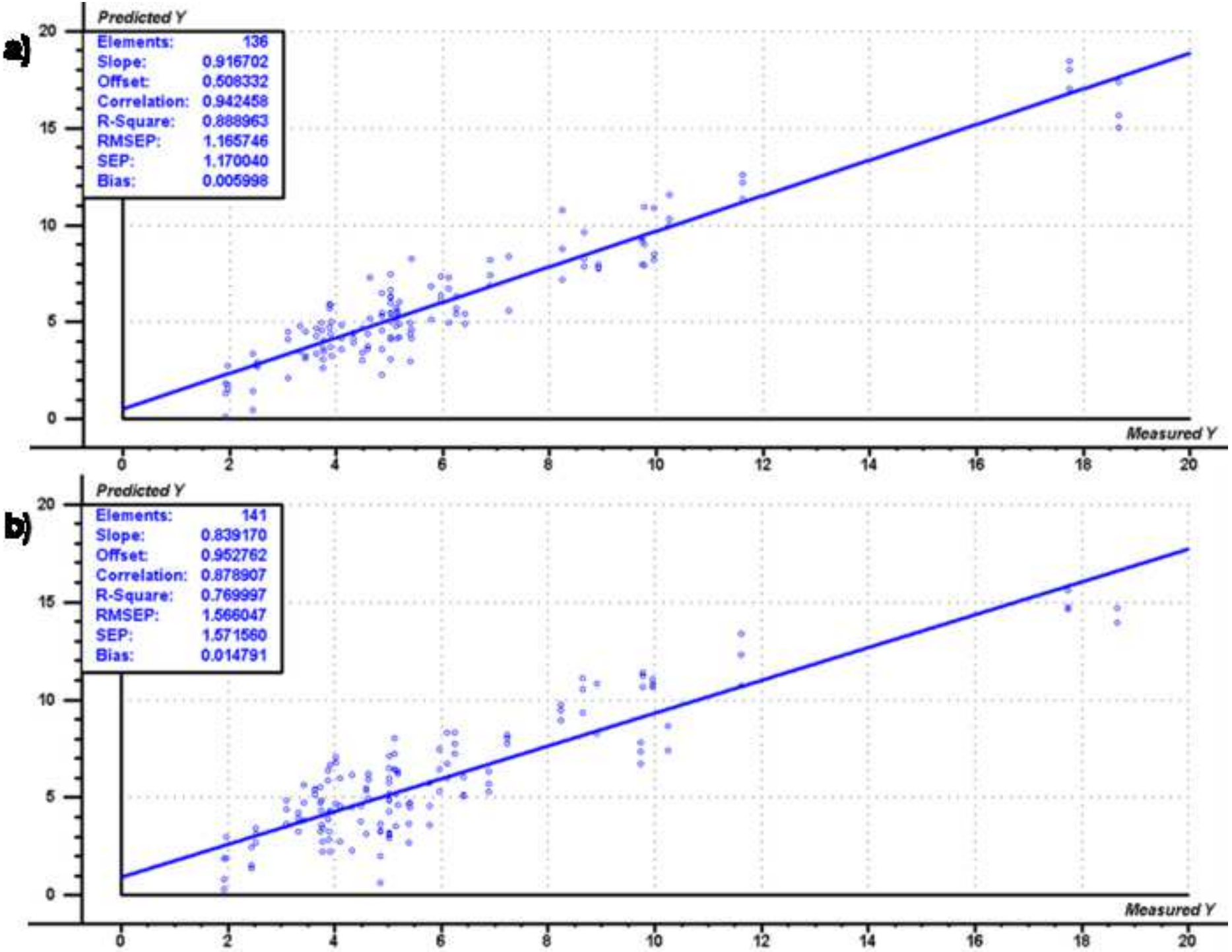

Figure 2

Click here to download high resolution image

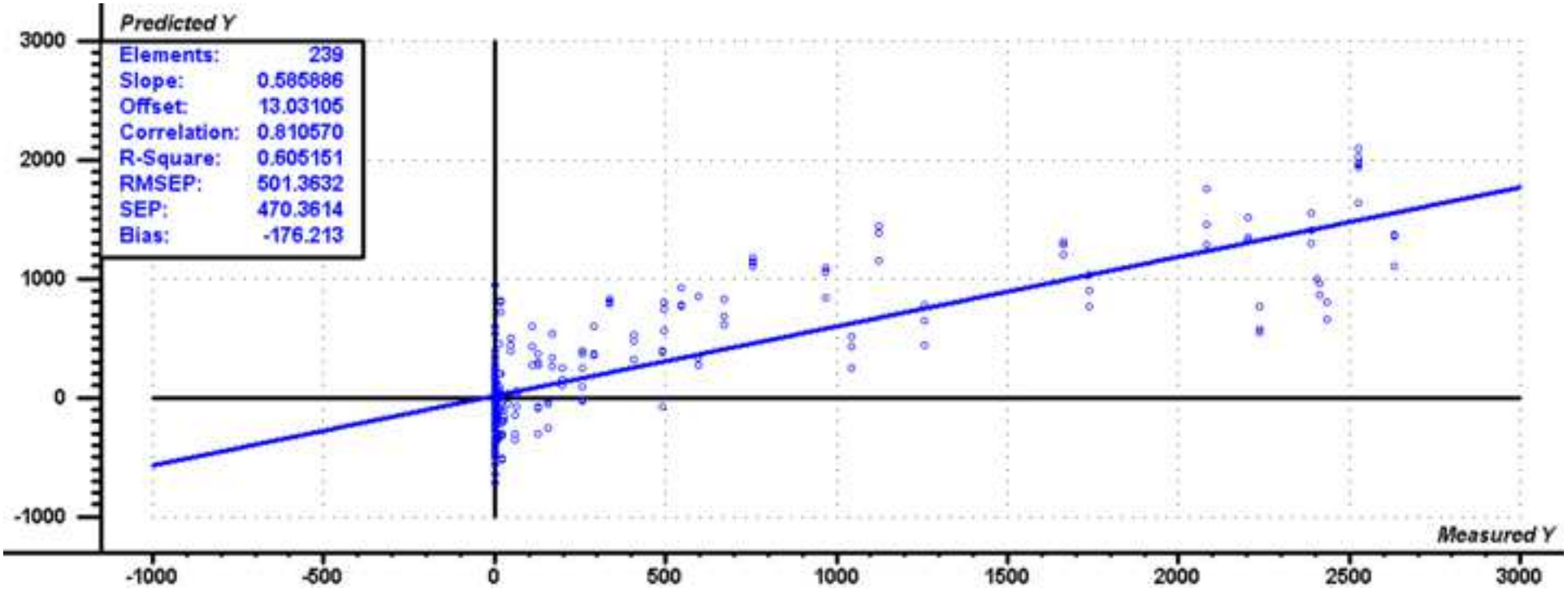

Figure 3

Click here to download high resolution image

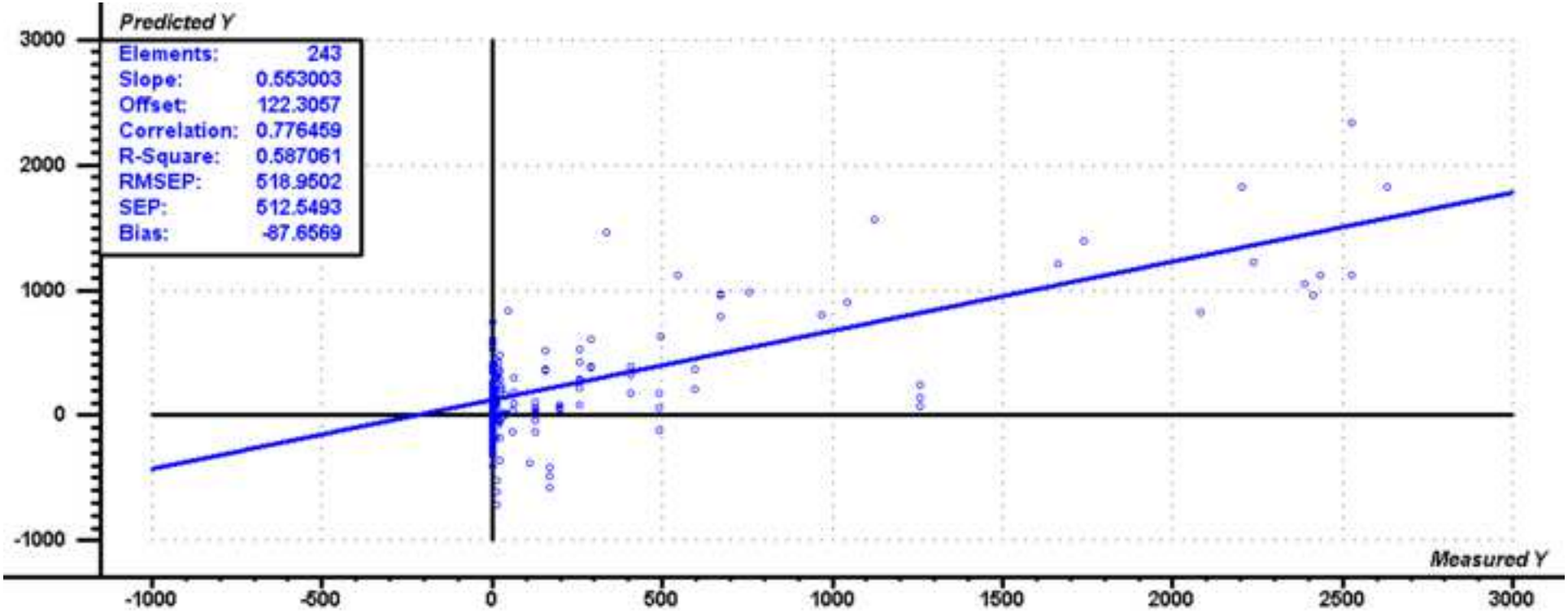

Supplementary material

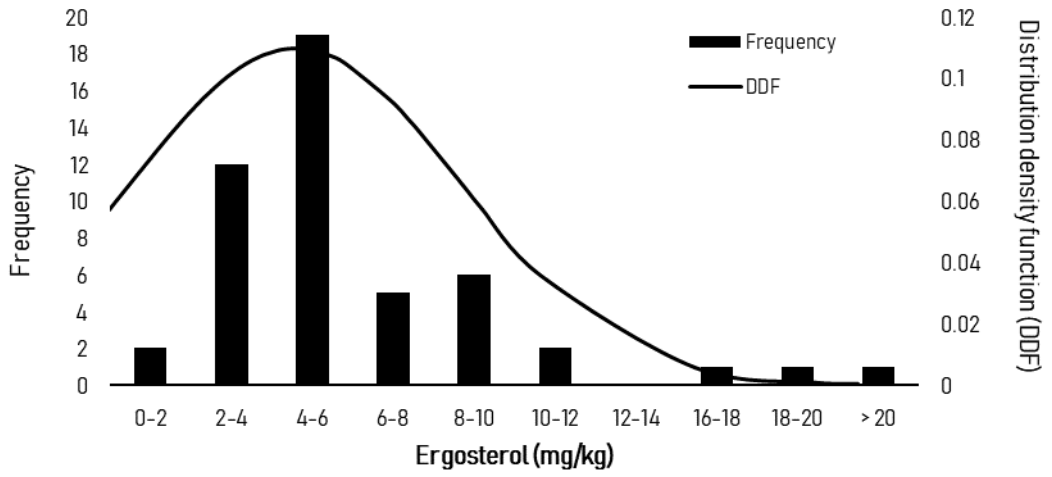

Figure S1. Distribution of total ergosterol content in single wheat kernels, on the full dataset used in the present experiments.

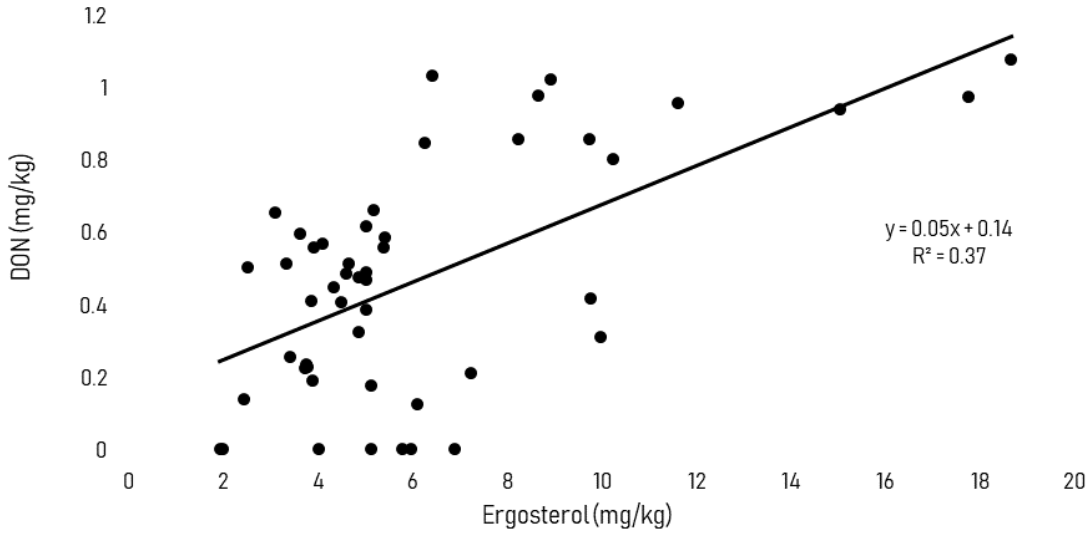

Figure S2. Correlation between DON concentration (Y) and ergosterol concentration (X).

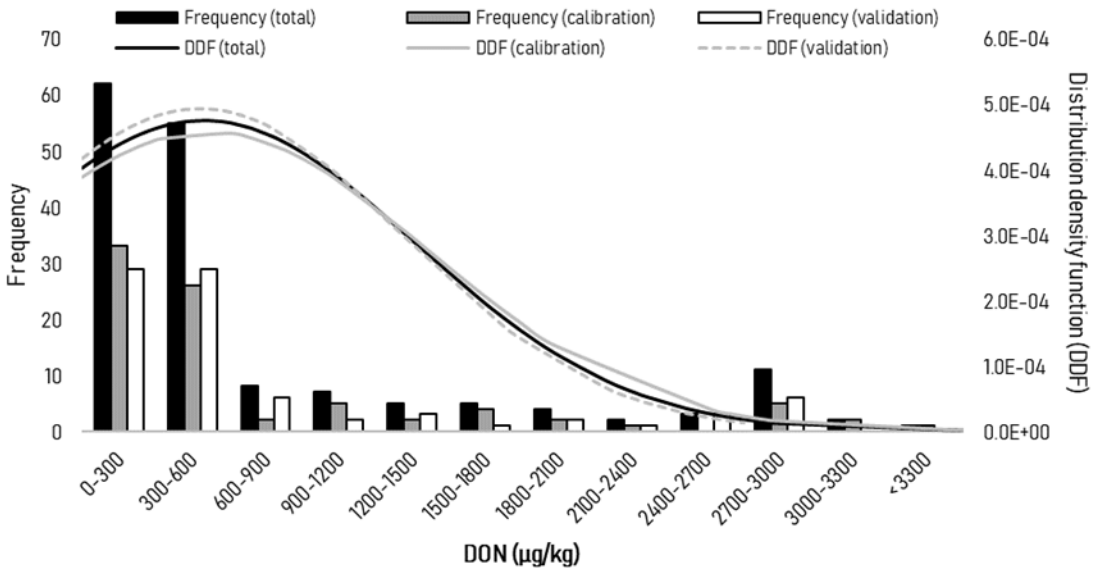

		No. of samples	Mean	Range	SDev	CV (%)
DON content (µg/kg)	**Calibration data set**	83	497.7	< 50 – 3537.0	873.7	175.5
	Validation data set	82	467.1	< 50 – 2628.5	807.8	172.9

Figure S3. Distribution of total DON content in wheat samples, on the full dataset used in the present experiments, and separately for the calibration and validation sets. Statistical analysis of the parameters of the samples used for DON models building, showing independently calibration and validation sets.

Table S1. Linear discriminant analysis (LDA) accuracies for the cross-validated model in unground samples.

Cross-validated set				
		Predicted		Accuracy (%)
Raw spectra	Groups	B	C	84.65
	B	341	70	
	C	6	78	
ABS/BC	Groups	B	C	83.64
	B	336	75	
	C	6	78	
1st Derivative	Groups	B	C	95.66
	B	393	18	
	C	4	80	

B = low-contaminated group of samples (< 1250 µg/kg); C = high-contaminated group of samples (> 1250 µg/kg). Grey cells indicate the number of correctly-classified samples. White cells indicate the number of miss-classified samples.

Table S2. Linear discriminant analysis (LDA) accuracies for a cross-validated model (threshold 1250 µg/kg) in ground samples.

Cross-validated set				
		Predicted		Accuracy (%)
Raw spectra	Groups	B	C	94.35
	B	389	22	
	C	6	78	
ABS/BC	Groups	B	C	84.05
	B	341	70	
	C	9	75	
1st Derivative	Groups	B	C	97.18
	B	400	11	
	C	3	81	

B = low-contaminated group of samples (< 1250 µg/kg); C = contaminated group of samples (> 1250 µg/kg). Grey cells indicate the number of correctly-classified samples. White cells indicate the number of miss-classified samples.

***Declaration of Interest Statement**

Declaration of interests

☒ The authors declare that they have no known competing financial interests or personal relationships that could have appeared to influence the work reported in this paper.

☐The authors declare the following financial interests/personal relationships which may be considered as potential competing interests: